## Supplemental Material: A diatom extension of the cGEnIE Earth system model – EcoGEnIE 1.1

EcoGEnIE 1.1 is a trait-based functional type ecosystem model developed from EcoGEnIE 1.0 (Ward et al., 2018) to include diatom dynamics and silicon cycle in the Earth System model, cGEnIE. EcoGEnIE 1.0 captured the dynamic of size classes of phytoplankton and zooplankton based on allometric relationships for, e.g., uptake rate, grazing rate and nutrient affinity. EcoGEnIE 1.1 depicts three new functional phytoplankton groups: picoplankton, eukaryote and diatom, each with two to three size classes relevant to their type (Table S1). To distinguish the different groups of phytoplankton, we used the allometric relationships as defined by Dutkiewicz et al. (2020) for the maximum photosynthetic rate for picoplankton and diatoms (Table S1).

| | **EcoGEnIE 1.0**<br>*(Ward et al., 2018)* | **EcoGEnIE 1.1**<br>*This study* |
|---|---|---|
| ECOSYSTEM | | |
| Ecosystem structure | 8 size classes of phytoplankton and zooplankton (0.6, 1.9, 6.0, 19.0, 60.0, 190.0, 600.0, 1900.0) | 3 size classes of diatoms (2.0, 20.0, 200.0)<br>2 size classes of picoplankton (0.6, 2.0)<br>2 size classes of eukaryote (20.0, 200.0)<br>4 size classes of zooplankton (6.0, 20.0, 200.0, 2000.0) |
| Maximum photosynthetic rate | Unimodal relationship for all plankton | Diatoms : $3.9V^{-0.08}$ d-1 (Dutkiewicz et al., 2020)<br>Picoplankton : $0.9V^{0.08}$ $d^{-1}$ (Dutkiewicz et al., 2020)<br>Eukaryotes: $2.2V^{-0.08}$ $d^{-1}$ (assuming 20% lower than diatoms) |
| Diatom trade-offs | N/A | Benefits: Higher Pmax and grazing protection<br>Cost: Si requirement |
| Light limitation | | Modified EcoGEnIE 1.0 with diagnosed mixed-layer light penetration and no light under sea-ice |
| BIOGEOCHEMISTRY | | |
| Iron cycle | Dust source: (Mahowald et al., 1999)<br>TDFe and TL<br>DOMτ = 1<br>Fesol = 1<br>Kscav = 1.338 | Dust source: Albani et al. (2016)<br>TDFe and TL<br>DOMτ = 0.5<br>Fesol = 0.00244<br>Kscav = 0.225 |
| Silicon cycle | N/A | bg_par_bio_red_POC_opal=0.65<br>bg_ctrl_bio_remin_opal_fixed=.false.<br>bg_par_bio_remin_sinkingrate=125.0 |

| | | |
|---|---|---|
| Extend the temperature range for solubility and geochemical constants | N/A | gm_par_geochem_Tmin = -2.0<br>gm_par_geochem_Tmax = 45.0<br>gm_par_carbchem_Tmin = -2.0<br>gm_par_carbchem_Tmax = 45.0 |
| Instantaneous remineralisation | N/A | bg_par_bio_remin_sinkingrate_physical=9.9E9;<br>bg_par_bio_remin_sinkingrate_reaction=125.0 |
| Geochemical reaction timescale | N/A | bg_par_bio_geochem_tau=90.0 |
| Relative partitioning of C into DOM | N/A | eg_par_beta_POCtoDOC=0.75 |
| PHYSICS | | |
| Configuration | Worlg4 (Worjh2 with modified wind) | Worjh2 (Cao et al., 2009) |
| Mixed-layer scheme | On | Off |

Table S1: EcoGEnIE 1.1 model setup in comparison to EcoGEnIE 1.0

## Plankton physiology

State variables and their rates of change are defined by a variety of ecological processes. Further state variables are fully described in Ward et al. (2018).

## Temperature limitation

Metabolic processes within cells are temperature limited. We account for temperature limitation applying the following exponential function of temperature to all plankton.

$$\gamma^T = e^{A(T-T_{ref})} \quad (1)$$

Temperature sensitivity is described by the constant $A$, $T$ is ambient water temperature in $^{o}$C and $T_{ref}$ is a reference temperature where $\gamma^T = 1$.

## Nutrient uptake

Environmental availability ($[R_{i_r}]$) of a nutrient ($i_r = i_b$) governs phytoplankton uptake rate, along with maximum uptake rate ($V^{max}$), quota saturation term, temperature limitation and nutrient affinity ($\alpha_{j,i_r}$).

$$V_{j,i_r} = \frac{V_{j,i_r}^{max} \alpha_{j,i_r}[R_{i_r}]}{V_{j,i_r}^{max} + \alpha_{j,i_r}[R_{i_r}]} Q_{j,i_b}^{stat} \cdot \gamma^T \quad (2)$$

This equation modifies the Michaelis-Menten-type response by including nutrient affinity rather than the half saturation constant.

## Plankton "quota" saturation

Saturation of nutrient biomass relative to carbon is prevented by setting the uptake capacity to zero when the cellular nutrient quota, $Q$, is satisfied (Ward et al., 2012). This quota is determined by the ratio of nutrients assimilated to carbon biomass.

$$Q_{j,i_b}^{stat} = \left(\frac{Q_{j,i_b}^{max} - Q_{j,i_b}}{Q_{j,i_b}^{max} - Q_{j,i_b}^{min}}\right)^h \quad (3)$$

The general uptake regulation term, $i_b$, for a given element $j$ is a linear function of the nutrient status, which is altered by the shape parameter $h = 0.1$ (Geider et al., 1998).

## Photosynthesis

We use a photosynthesis model for phytoplankton adapted from Geider et al. (1998) and Moore et al. (2001) where light limitation ($\gamma_{j,I}$) relates to the Poisson function. This function depends on local irradiance ($I$) depends on the chlorophyall $a$: carbon ratio ($Q_{j:Chl}$) and iron-dependent initial slope of the $P$-$I$ curve ($\alpha \cdot \gamma_{j,Fe}$).

$$\gamma_{j,I} = 1 - \exp\left(\frac{-\alpha \cdot \gamma_{j,Fe} \cdot Q_{j,Chl} \cdot I}{P_{j,C}^{sat}}\right) \quad (4)$$

$P^{sat}$ refers to the maximum light-saturated growth rate, which depends on a maximum rate of $P^{max}$ with respect to the temperature and nutrient limitations.

$$P_{j,C}^{sat} = P_{j,C}^{max} \cdot \gamma^T \cdot \min\left[\gamma_{j,P}, \gamma_{J,Fe}\right] \quad (5)$$

The resulting gross photosynthetic growth rate ($P_{j,C}$) is thus calculated as:

$$P_{j,C} = \gamma_{j,I} P_{j,C}^{sat} \quad (6)$$

## Grazing

We determine a predator's ($j_{pred}$) predator-biomass specific grazing rate on its prey ($j_{prey}$) by the overall grazing rate, the prey switching term ($\phi$) and prey refuge ($1 - e^{\Lambda \cdot F_{j_{pred},C}}$) where grazing will reduce if availability is low.

$$G_{j_{pred},j_{prey},C} = \gamma^T \cdot G_{j_{pred},C}^{max} \cdot \frac{F_{j_{pred},C}}{k_{j_{prey},C} + F_{j_{pred},C}} \cdot \phi_{j_{pred},j_{prey}} \cdot \left(1 - e^{\Lambda \cdot F_{j_{pred},C}}\right) \quad (7)$$

$G^{max}$ represents the maximum grazing rate, with a half-saturation concentration for all prey denoted $k_{jprey,C}$ and total available food as $F_{jpred,C}$. The "prey-switching" term is optional with the details outlined in Ward et al. (2018). We assume that predators do not feed on detrital organic matter.

## Mortality

Biomass loss also occurs via mortality via a linear biomass mortality rate ($m_j$).

$$m_j = m_p \left(1 - e^{-10^{10} \cdot B_{j,C}}\right) \quad (8)$$

$m_j$ reduces when population carbon biomass (represented by the vector $B_C$) is smaller than $10^{-10}$ mmol C $m^{-3}$, to help support low biomass population to ensure that every surface grid cell houses a viable population.

## Other plankton distribution

The carbon biomass distributions of the base functional types of our plankton community and their grazers (zooplankton) are shown in Figure S1 and S2. Global distributions of 0.6 μm picoplankton are generally consistent across high and low latitudes, with subtropical gyres housing far less of the 2 μm class. Eukaryotes, being of the micro size, exhibit distinct regions of habitancy relative to picoplankton, their larger 200 μm class is restricted to high latitudes whilst the 20 μm class also emanates in equatorial zones. Respective zooplankton size classes are intuitively determined by the presence of their prey (i.e. groups at least 10 times smaller than them), thus we observe larger zooplankton occupying increasingly smaller ecological niches.

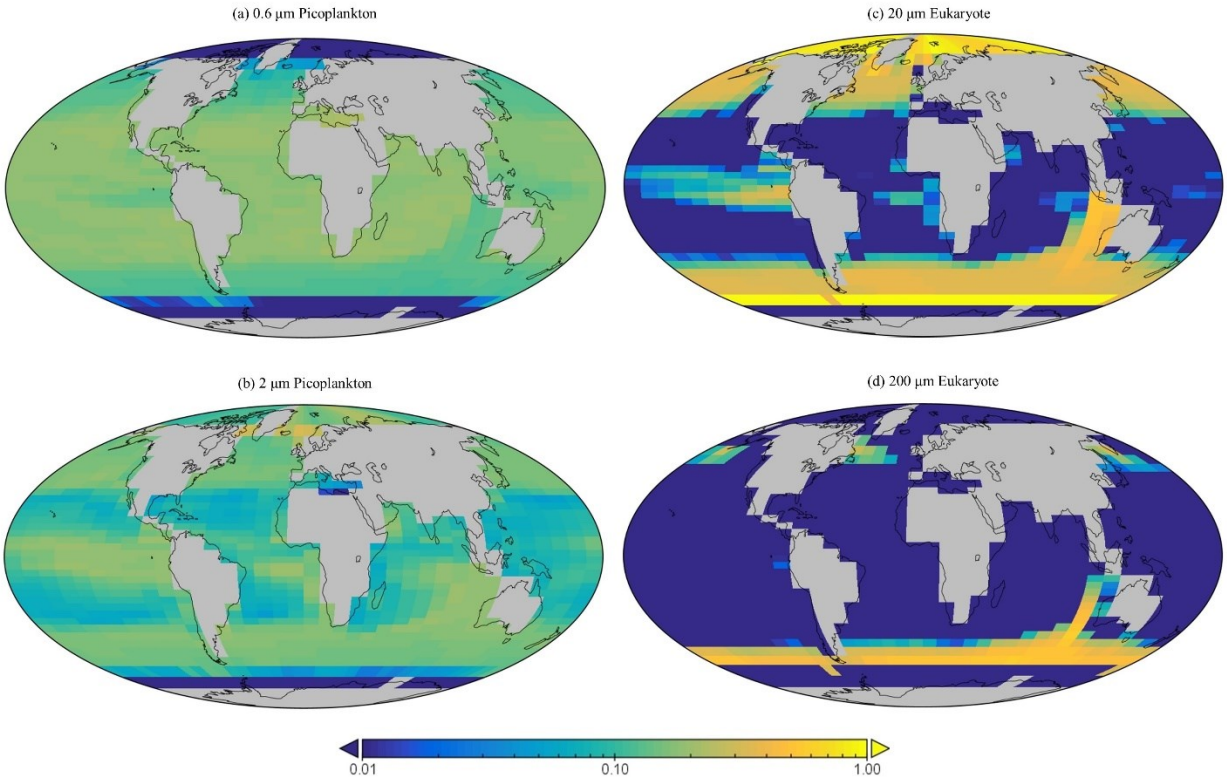


**Figure S1.** Surface concentrations of carbon biomass for picoplankton ((a) and (b)), and eukaryotes ((c) and (d)) size classes (mmol C $m^{-3}$).

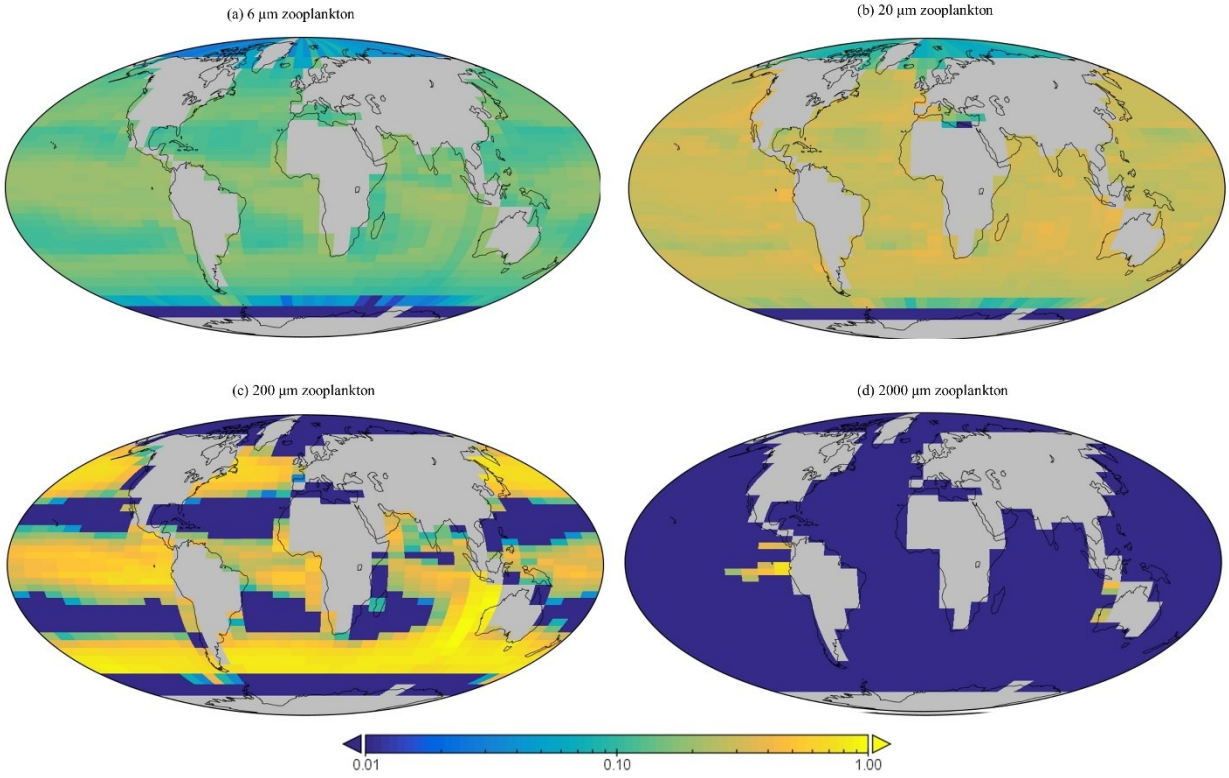


**Figure S2.** Surface concentrations of carbon biomass for each zooplankton size class (mmol C $m^{-3}$).

**M-score trade-off**

Figure S3 shows a trade-off in oxygen and phosphate M-scores, a factor we took into consideration when selecting our best run.

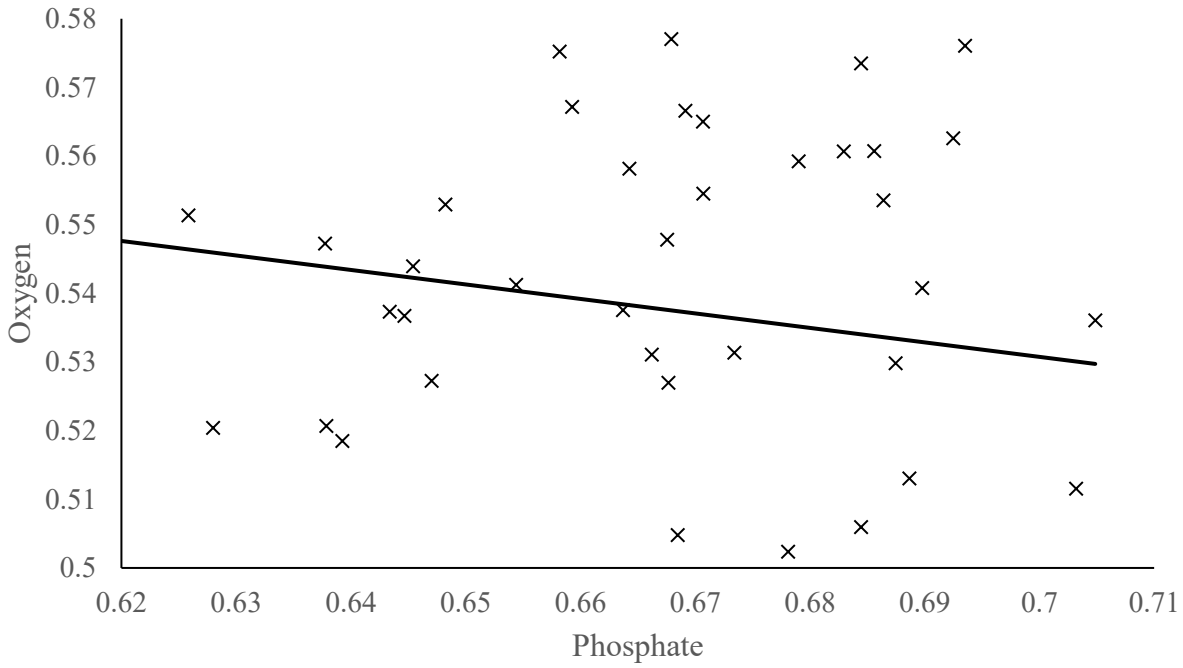


**Figure S3.** Top 50 average M-score runs with oxygen and phosphate plotted against each other.

**Supplemental References**

Albani, S., Mahowald, N. M., Murphy, L. N., Raiswell, R., Moore, J. K., Anderson, R. F., McGee, D., Bradtmiller, L. I., Delmonte, B., Hesse, P. P., and Mayewski, P. A.: Paleodust variability since the Last Glacial Maximum and implications for iron inputs to the ocean, Geophysical Research Letters, 43, 3944-3954, 10.1002/2016gl067911, 2016.

Cao, L., Eby, M., Ridgwell, A., Caldeira, K., Archer, D., Ishida, A., Joos, F., Matsumoto, K., Mikolajewicz, U., Mouchet, A., Orr, J. C., Plattner, G. K., Schlitzer, R., Tokos, K., Totterdell, I., Tschumi, T., Yamanaka, Y., and Yool, A.: The role of ocean transport in the uptake of anthropogenic CO<sub>2</sub>, Biogeosciences, 6, 375-390, https://doi.org/10.5194/bg-6-375-2009, 2009.

Dutkiewicz, S., Cermeno, P., Jahn, O., Follows, M. J., Hickman, A. E., Taniguchi, D. A. A., and Ward, B. A.: Dimensions of marine phytoplankton diversity, Biogeosciences, 17, 609-634, 10.5194/bg-17-609-2020, 2020.

Geider, R. J., Maclntyre, H. L., and Kana, T. M.: A dynamic regulatory model of phytoplanktonic acclimation to light, nutrients, and temperature, Limnology and Oceanography, 43, 679-694, 10.4319/lo.1998.43.4.0679, 1998.

Mahowald, N., Kohfeld, K., Hansson, M., Balkanski, Y., Harrison, S. P., Prentice, I. C., Schulz, M., and Rodhe, H.: Dust sources and deposition during the last glacial maximum and current climate: A comparison of model results with paleodata from ice cores and marine sediments, Journal of Geophysical Research: Atmospheres, 104, 15895-15916, 10.1029/1999jd900084, 1999.

Moore, J. K., Doney, S. C., Kleypas, J. A., Glover, D. M., and Fung, I. Y.: An intermediate complexity marine ecosystem model for the global domain, Deep Sea Research Part II: Topical Studies in Oceanography, 49, 403-462, 10.1016/s0967-0645(01)00108-4, 2001.

Ward, B. A., Dutkiewicz, S., Jahn, O., and Follows, M. J.: A size-structured food-web model for the global ocean, Limnology and Oceanography, 57, 1877-1891, 10.4319/lo.2012.57.6.1877, 2012.

Ward, B. A., Wilson, J. D., Death, R. M., Monteiro, F. M., Yool, A., and Ridgwell, A.: EcoGEnIE 1.0: plankton ecology in the cGEnIE Earth system model, Geosci. Model Dev., 11, 4241-4267, https://doi.org/10.5194/gmd-11-4241-2018, 2018.